Supplemental Figures and Legends

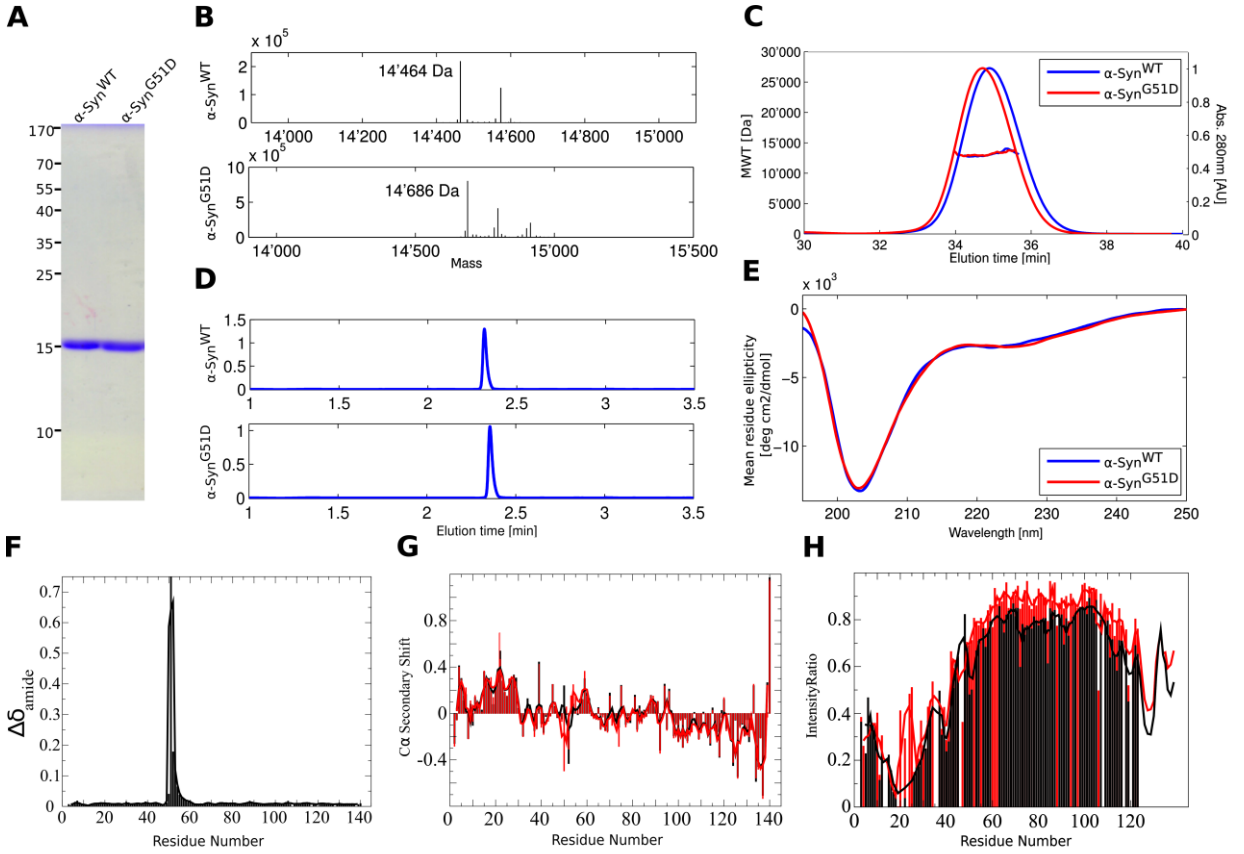

Supplemental figure 1. Characterization and purity analysis of α-Syn^{WT} and mutant. (A) SDS PAGE of recombinant α-Syn^{WT} and α-Syn^{G51D} shows that both proteins run as a single monomeric band. **(B)** ESI-MS indicates the correct masses (expected masses are 14'461Da for α-Syn^{WT}, and 14'519Da for α-Syn^{G51D}). **(C)** Multi-angle light scattering. Both proteins show monomeric elution profiles. The calculated masses are: α-Syn^{WT}: 13.18 KDa (+/-3%), α-Syn^{G51D}: 13.15 KDa (+/-4%). **(D)** UPLC analysis of recombinant proteins; single, sharp and symmetrical peaks are obtained. **(E)** Circular dichroism confirms the random coil conformation of WT and G51D α-Syn. **(F)** Plot of averaged amide chemical shift difference [$\Delta\delta_{amide} = \sqrt{(½(\Delta\delta_{HN}^2 + (\Delta\delta_N/5)^2))}$] between the free state α-Syn^{G51D} and α-Syn^{WT} spectra as a function of residue number. The lines show 3-residue averages. **(G)** Plot of alpha-carbon secondary shifts (difference between measured chemical shift and random coil chemical shift) for α-Syn^{WT} (black) and α-Syn^{G51D} (red) in aqueous buffer by residue number. The lines show 3-residue averages. **(H)** Plot of ratio of cross-peak intensity of samples spin-labeled at position 20 to samples without spin-label for α-Syn^{WT} (black) and α-Syn^{G51D} (red), in aqueous buffer by residue number. The lines show 3-residue averages.

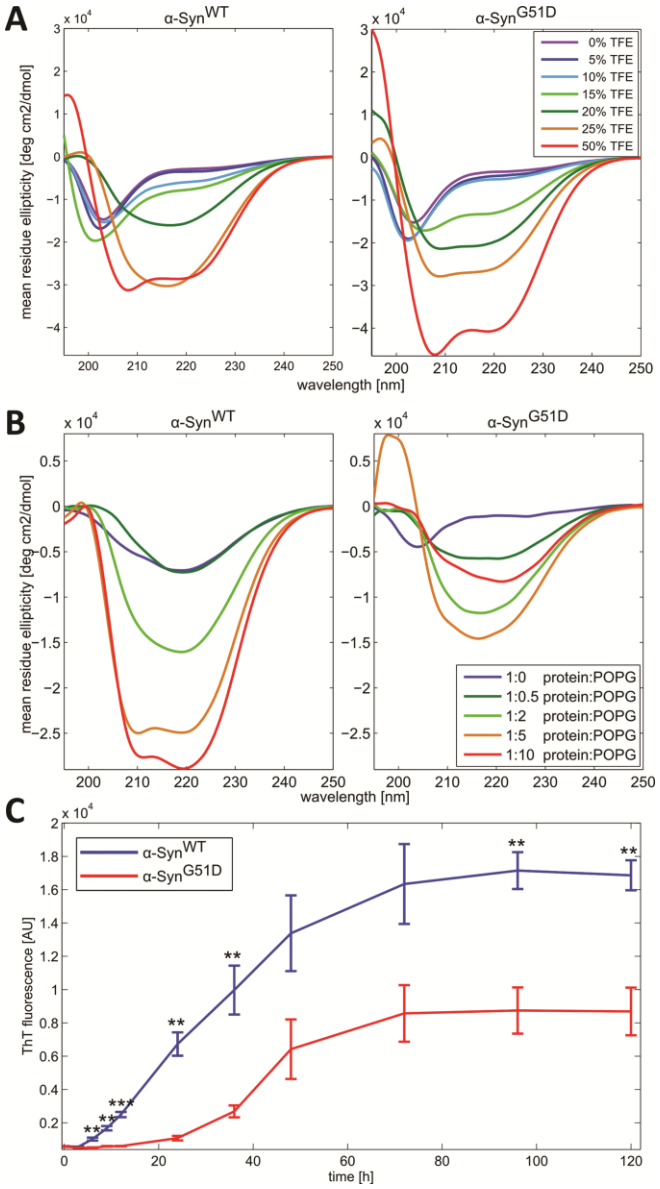

Supplemental figure 2. Both α-Syn^{WT} and α-Syn^{G51D} form α-helices when incubated with TFE. (A) Circular dichroism of α-Syn^{WT} and α-Syn^{G51D} mixed with different percentages of TFE. Both proteins form α-helices in the presence of high TFE percentage, demonstrating the inherent ability of both WT and mutant α-Syn to form α-helices in a membrane-mimicking environment. **(B)** Circular dichroism of α-Syn^{WT} and α-Syn^{G51D} mixed with protein:lipid weight ratios of 1:0, 1:0.5, 1:2, 1:5 and 1:10, and incubated for 24h at 37°C under shaking conditions. At high POPG content, formation of β-sheet is inhibited in the case of the WT protein, due to the strong α-helical conformation. **(C)** Kinetics of aggregation of 100µM α-Syn^{WT} and α-Syn^{G51D} followed by ThT +/- S.E.M (*: p-value<0.05, **: p-value<0.01, ***: p-value<0.001, n=3). Similarly to the experiments performed at 10µM, the G51D mutant shows a longer lag phase and reaches a lower plateau ThT value.

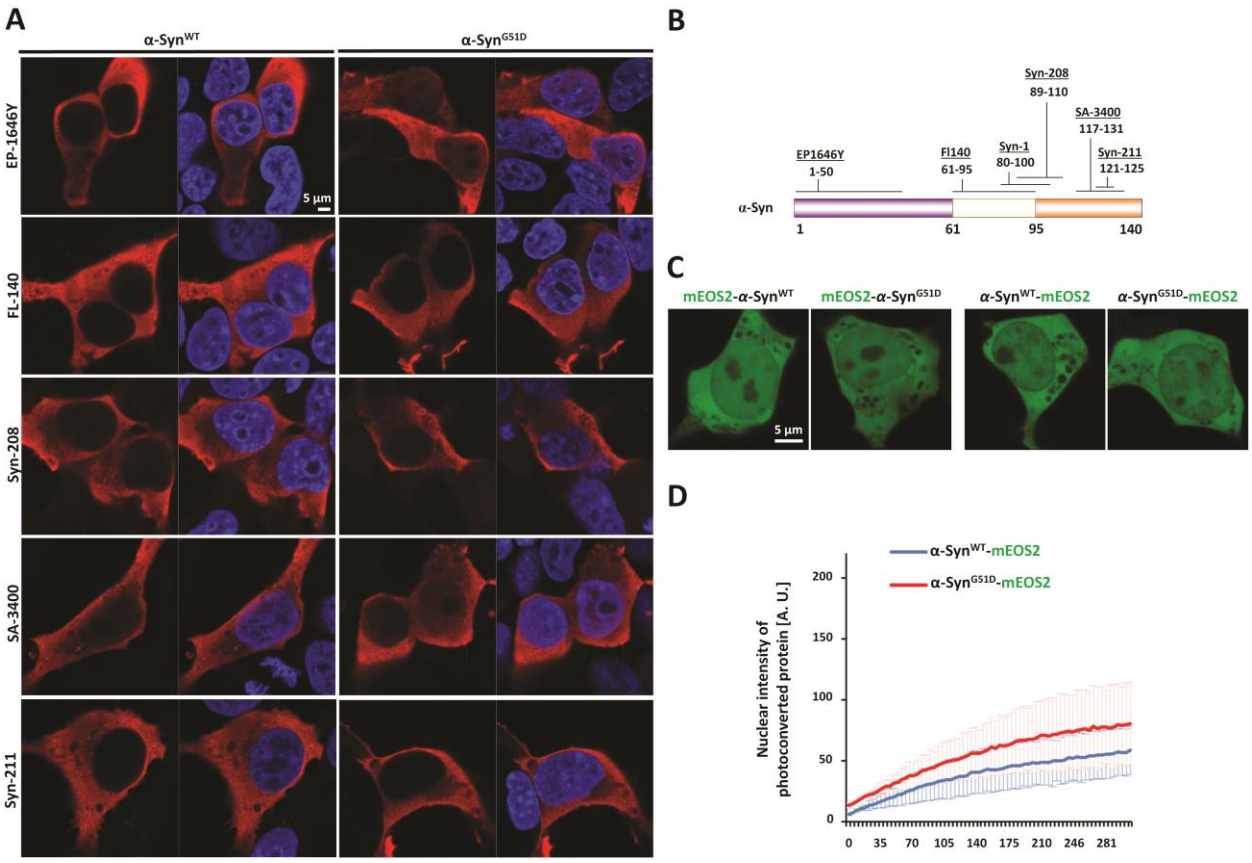

Supplemental figure 3. Detection of nuclear α-Syn by immunocytochemistry and live imaging in HEK cells. (A) Immunocytochemical analysis of HEK cells expressing α-Syn^{WT} or α-Syn^{G51D} using different antibodies targeting α-Syn shows that unlike the Syn208, Syn211, and FL-140 antibodies, the EP-1646Y, SA3400 and Syn-1 (shown in Figure 3) antibodies efficiently detect nuclear α-Syn. **(B)** Scheme depicting the α-Syn protein and the epitopes of the antibodies tested in (A) and in Figure 1. **(C)** Live imaging of HEK cells transfected with WT or G51D mEOS2-α-Syn (left panel) or α-Syn-mEOS2 (right panel) shows that all expressed proteins show cytoplasmic and nuclear localization. **(D)** Fluorescence intensity curves of nuclear photoactivated WT or G51D α-Syn-mEOS2 in cells photoconverted in the cytosol. For each condition, at least 25 cells were analyzed. Each plot represents mean ± SD for each time point of all photoactivation experiments.

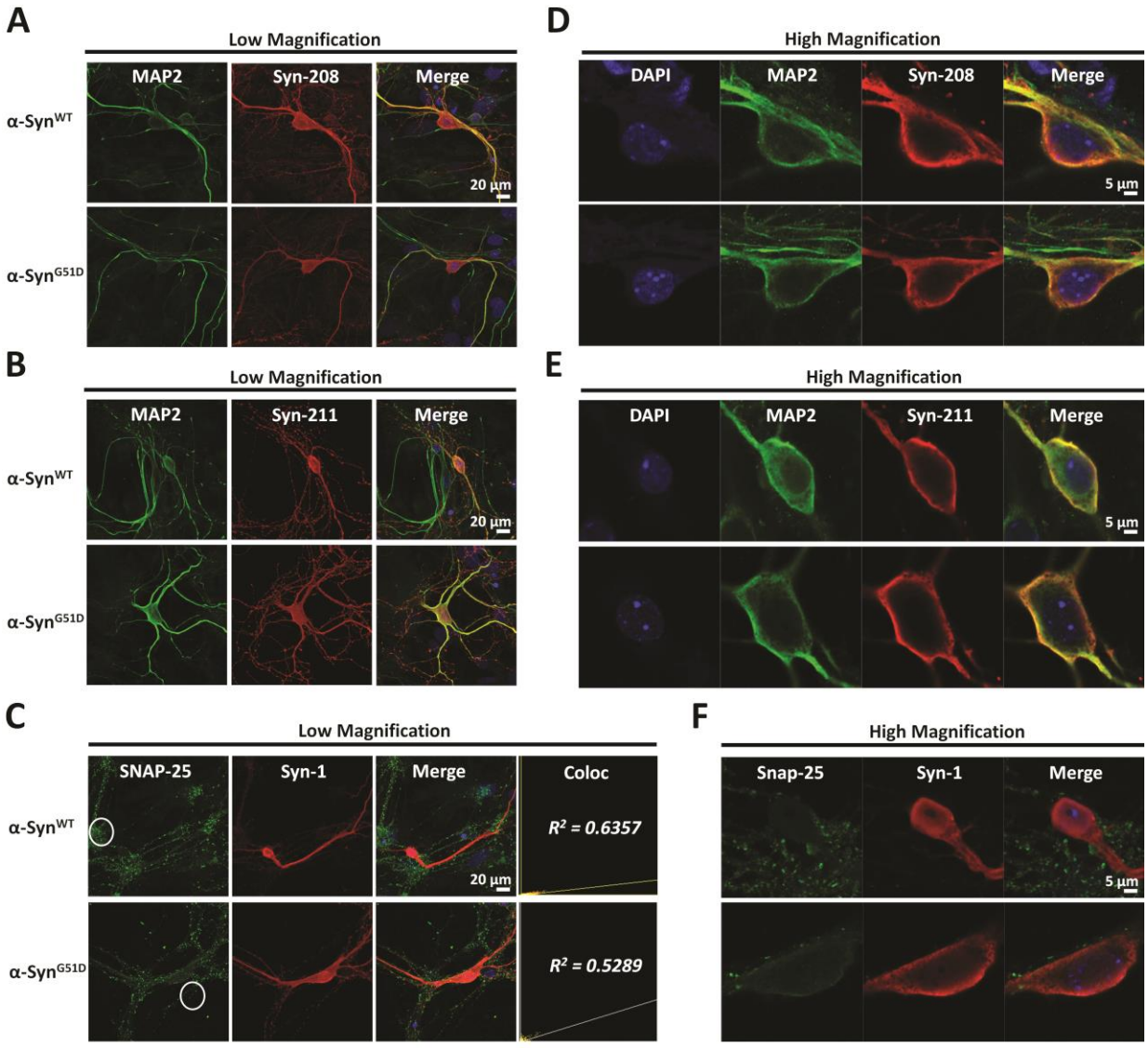

Supplemental figure 4. Detection of nuclear α-Syn by immunocytochemistry in primary neurons. Immunocytochemical analysis of neurons expressing α-Syn^{WT} or α-Syn^{G51D} shows that all tested antibodies (Syn-208, Syn-211 and Syn-1) detect α-Syn in neuronal soma and neurites **(A-C,** low magnification images**)**. However, whereas the Syn-208 **(D)** and Syn-211 **(E)** antibodies detect only cytosolic α-Syn within soma, the Syn-1 antibody detects additional nuclear signal in both WT and α-Syn^{G51D} expressing neurons **(F)**. MAP2 and SNAP-25 were used as markers to delineate neurons **(A, B, D, E)**, and presynaptic terminals **(C, F)** respectively. Note that in **(C)**, colocalization analysis was performed on a circular region of interest (white circle) having neuritic expression of α-Syn to establish colocalization with SNAP-25.

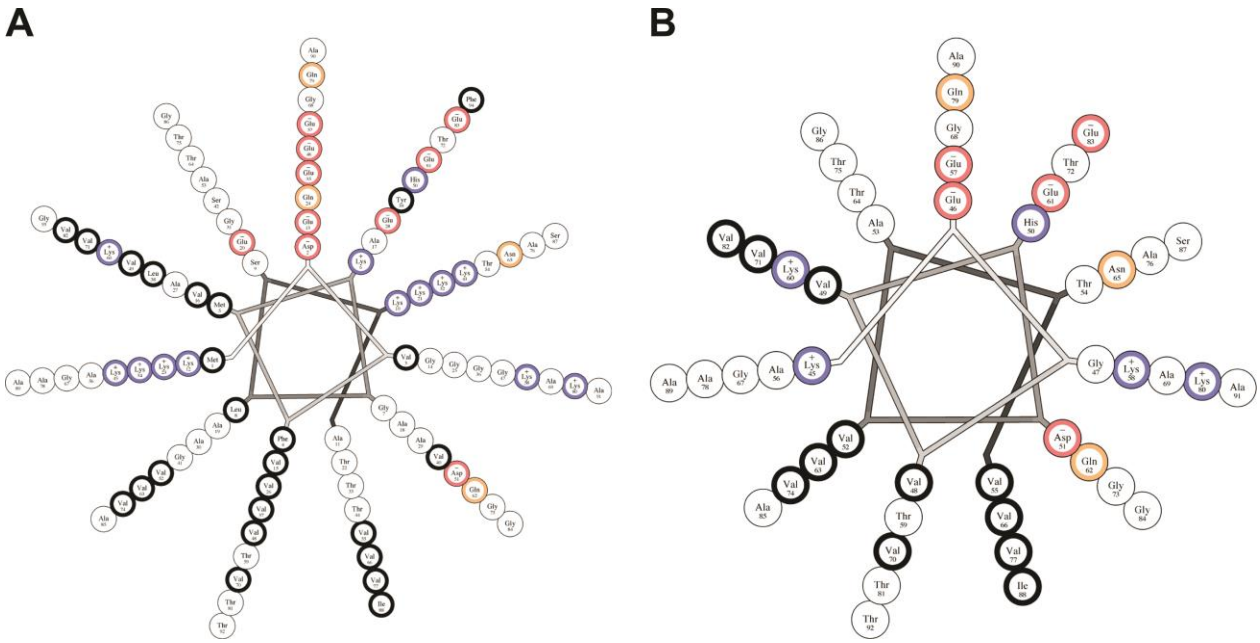

Supplemental figure 5. Helical wheel representation of α-Syn^{G51D} extended and broken helix conformations. Basic residues are in blue, acidic residues in pink, amide residues in orange and hydrophobic residues in black. **(A)** When α-Syn^{WT} binds to lipid vesicles, it adopts an extended 11/3 α-helix conformation. By introducing a charged residue into the apolar face of the amphipathic α-helix, the G51D mutation might perturb its capacity to interact with the hydrophobic phospholipid tails. **(B)** In the presence of SDS, the N-terminal region of α-Syn^{WT} forms a broken-helix made of two antiparallel helices connected by a short linker (1-4). The G51D mutation introduces a negative charge in the apolar face of the helix-2 (2, 4), which might perturb the ability of this region to interact with the hydrophobic interior of the detergent micelle.

Supplemental Tables

Table S1: List of antibodies used in this study.

	Antibody	Source/Reference	Dilution
Anti α-Syn	Syn-211	Santa Cruz	1:1000
	FL-140	Santa Cruz	1:750
	N-19	Santa Cruz	1:100
	Syn-1	BD lab	1:1000
	EP-1646Y	Abcam	1:750
	Syn-208	Virginia Lee, University of Pennsylvania, CNDR, Philadelphia,PA) (5, 6)	1:500
	SA3400	Millipore	1:750
	pS129 α-Syn	WAKO	1:2000
	pS129 α-Syn	MJF-R13	1:1000
Other	SNAP-25	Cell Signaling	1:1000
	MAP-2	Cell Signaling	1:750
	GRK6	Santa Cruz	1:1000
	Flag	Abcam	1:1000
	Actin	Abcam	1:5000

References

1 Borbat, P., Ramlall, T.F., Freed, J.H. and Eliezer, D. (2006) Inter-helix distances in lysophospholipid micelle-bound alpha-synuclein from pulsed ESR measurements. *J Am Chem Soc*, **128**, 10004-10005.

2 Bussell, R., Jr. and Eliezer, D. (2003) A structural and functional role for 11-mer repeats in alpha-synuclein and other exchangeable lipid binding proteins. *J Mol Biol*, **329**, 763-778.

3 Chandra, S., Chen, X., Rizo, J., Jahn, R. and Sudhof, T.C. (2003) A broken alpha -helix in folded alpha -Synuclein. *J Biol Chem*, **278**, 15313-15318.

4 Ulmer, T.S., Bax, A., Cole, N.B. and Nussbaum, R.L. (2005) Structure and dynamics of micelle-bound human alpha-synuclein. *J Biol Chem*, **280**, 9595-9603.

5 Tsika, E., Moysidou, M., Guo, J., Cushman, M., Gannon, P., Sandaltzopoulos, R., Giasson, B.I., Krainc, D., Ischiropoulos, H. and Mazzulli, J.R. (2010) Distinct region-specific alpha-synuclein oligomers in A53T transgenic mice: implications for neurodegeneration. *J Neurosci*, **30**, 3409-3418.

6 Giasson, B.I., Duda, J.E., Quinn, S.M., Zhang, B., Trojanowski, J.Q. and Lee, V.M. (2002) Neuronal alpha-synucleinopathy with severe movement disorder in mice expressing A53T human alpha-synuclein. *Neuron*, **34**, 521-533.